Journal of Thermal Analysis Vol. 46 (1996) 935-954

Dedicated to Professor Bernhard Wunderlich on the occasion of his 65th birthday

TEMPERATURE MODULATED CALORIMETRY AND DIELECTRIC SPECTROSCOPY IN THE GLASS TRANSITION REGION OF POLYMERS

A. Hensel, J. Dobbertin, J. E. K. Schawe[1], A. Boller[2] and C. Schick

Universität Rostock, Fachbereich Physik, Universitätsplatz 3, D-18051 Rostock
[1]Universität Ulm, Sektion für Kalorimetrie, D-89069 Ulm, Germany
[2]University of Tennessee, Department of Chemistry, Knoxville, TN 37996-1600, USA

Abstract

The results from temperature modulated DSC in the glass transition region of amorphous and semicrystalline polymers are described with the linear response approach. The real and the imaginary part of the complex heat capacity are discussed. The findings are compared with those of dielectric spectroscopy. The frequency dependent glass transition temperature can be fitted with a VFT-equation. The transition frequencies are decreased by 0.5 to 1 orders of magnitude compared to dielectric measurements. Cooling rates from standard DSC are transformed into frequencies. The glass transition temperatures are also approximated by the VFT-fit from the temperature modulated measurements. The differences in the shape of the curves from amorphous and semicrystalline samples are discussed.

Keywords: calorimetry, dielectric, glass transition, modulated DSC, polymers, relaxation

Introduction

The glass transition is at present a central problem of condensed-matter physics, but there is no generally accepted theory for it. The glass transition is a universal phenomenon. It can be observed not only in ordinary silicate glasses, but also in materials with conformational mobility such as polymers, low molecular weight liquids, and liquid, plastic or condis crystals [1].

Calorimetric investigation of glass forming materials yields a deeper insight into the complex molecular processes associated with the glass transition. The comprehensive activity of Wunderlich in the field of differential scanning calorimetry (DSC) resulted in a better understanding of some general aspects of the glass transition. For example, the universality of the contribution of 11 J mol^{-1} K^{-1} per mobile bead to the step in the specific heat capacity at the

0368–4466/96/ $ 5.00
© 1996 Akadémiai Kiadó, Budapest
John Wiley & Sons, Limited
Chichester

glass transition [2] or the introduction of a rigid amorphous fraction in semi-crystalline polymers [3], as well as the classification of the structure of matter compared with molecular mobility [1, 4, 5]. Wunderlich also discusses the relationship between the calorimetric glass transition (vitrification) and the dynamic glass transition (relaxation process) [6, 7]. We will develop this idea further in the present paper.

A very useful experimental method to probe a condensed matter system in the glass transition range is to measure the linear response of the system to a small external perturbation. Such experiments are e.g. dynamic-mechanic- or dielectric-spectroscopy. The general theoretical framework for the linear response was given by Kubo [8] in the case of relaxation processes. As shown by different authors, the specific heat capacity can also be described as a compliance in the linear response approach [9–11]. In general, heat capacity is a time or frequency dependent quantity. The commonly used static thermodynamic quantity is then the time- or ensemble-averaged one. In other words, we have to take into account the relationship between the time scale of the calorimetric experiment and the time scale of the processes under investigation. In the case of a glass transition, a pure relaxation phenomenon, it is well known that the thermal glass transition temperature (vitrification) depends on the cooling rate [12].

In a Temperature Modulated Differential Scanning Calorimetric (TMDSC) experiment the frequency of the modulation determines one time scale of the experiment and therefore the dynamic glass transition temperature [6, 7]. Taking into account the underlying cooling or heating rate, there is a second time scale in TMDSC due to the underlying rate. Therefore, we can investigate in one experiment the response to a small perturbation (from the modulated signal) as well as the vitrification (decreasing the average temperature) as in standard DSC experiments. This gives the opportunity to compare both time scales directly and to prove the rules for transforming cooling rates into frequencies, as proposed by Donth [13] or Stoll [14].

In this paper we compare the results of temperature modulated DSC in the frequency range from 0.08 Hz to 0.0003 Hz (12 to 3000 seconds period length) with that of standard DSC with cooling rates β in the range from 20 K min^{-1} to 0.6 K min^{-1} and with dielectric spectroscopy in the same frequency range.

Data evaluation and experimental details

Temperature modulated calorimetry* is a very useful tool for determination of the static heat capacity, especially at low temperatures, e.g. Sullivan and

* "Temperature modulated calorimetry" is used as the base term for all calorimetric methods using temperature modulation. "Temperature Modulated DSC" (TMDSC) is used for all calorimetric

Seidel [15]. Measurements of the frequency dependent specific heat capacity in the glass transition region of propylene glycol were first published by Birge and Nagel [16]. They used a so-called "third harmonic detection" to get information on the product of the complex specific heat capacity and thermal conductivity of a sample-heater assembly. Because there are different problems with the thermal contact between heater and sample, the "third harmonic detection" technique is a very interesting experimental method, but not a standard calorimetric method for everyday use.

Introducing the "Modulated Differential Scanning Calorimetry" (MDSC) by TA Instruments in 1992 [17] as an extension to normal DSC, TMDSC was available without big experimental problems. The data evaluation of this system was first described in [17, 18] and in detail by Wunderlich and co-workers [19, 20].

In this work we return to the linear response approach [8] and the data evaluation proposed by Schawe [11]. The linear response approach is a very general one and there is only one restriction concerning the shape of the external perturbation and the design of the apparatus used for the experiment. This restriction is that the perturbation is small, or in other words, the experiment must be linear. This means that the Boltzmann superposition principle must be valid [8]. Neglecting details, we can introduce an auto-correlation function $\Psi(t)$, dependent on the material properties which describes the relation between the change in time of an intensive variable of the system (e.g. temperature T) (perturbation) and the measured response of a time dependent extensive variable (e.g. enthalpy H). These quantities are connected by the convolution product [10, 11]

$$\partial H(t) = \int_{-\infty}^{t} \Psi(t - t')\, \partial T(t')\mathrm{d}t' \tag{1}$$

The convolution product can be solved by Fourier transformation, see [11] for details. According to Landau [9] a complex heat capacity can be introduced

$$C(\omega) = \int_{0}^{\infty} \Psi(t)\mathrm{e}^{\mathrm{i}\omega t}\mathrm{d}t \tag{2}$$

with

$$C(\omega) = C'(\omega) + iC''(\omega) \tag{3}$$

methods using temperature modulation and a differential measuring set-up, including measurements with an underlying heating or cooling ramp as well as quasi-isothermal experiments.

and

$$\omega = 2\pi\nu = \frac{2\pi}{t_p}$$

where ω is the angular frequency, ν is the frequency and t_p is the modulation period.

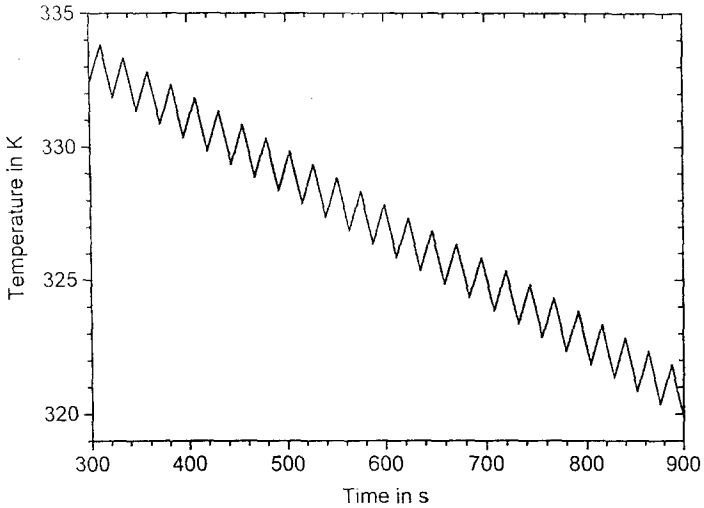

Fig. 1 Modulated temperature–time-function for the TMDSC heat-cool-mode. t_p = 24 s; T_a = 0.6 K; $<\beta> = -1.2$ K min^{-1}

The loss tangent can be determined according to:

$$\tan\delta(\omega) = \frac{C''(\omega)}{C'(\omega)} \tag{4}$$

From the modulated temperature and the measured modulated heat flow other quantities can be determined in addition. The reversing part of the heat capacity, as discussed by Reading [18] and Wunderlich [19] equals the modulus $|C(\omega)|$ of the complex heat capacity according to:

$$|C(\omega)| = \sqrt{(C'(\omega))^2 + (C''(\omega))^2} \tag{5}$$

The experiments were carried out with a modified Perkin Elmer DSC-7 (DDSC). The temperature–time-program consists of successive heating and cooling ramps (saw-tooth modulation Fig. 1). It is called the heat-cool-mode. The temperature–time-program can be written as a Fourier series:

$$T(t) = T_o + <\beta> t + \frac{4T_a}{\pi}\left[\frac{\sin \omega t}{1^2} - \frac{\sin 3\omega t}{3^2} + \frac{\sin 5\omega t}{5^2} - + \ldots\right] \quad (6)$$

where T_o is the starting temperature, $<\beta>$ is the underlying cooling or heating rate and T_a is the temperature amplitude.

The most dominant component of this Fourier series is the first term related to the first harmonic. There is no problem using Fourier analysis to extract the response to the first harmonic from the measured signal.

A small part of the temperature–time function for a typical experiment in the glass transition region of PVAc is shown in Fig. 1 and the corresponding measured heat flow in Fig. 2. From both curves, according to Eqs (1), (2), (3) and (4), the real (c') and the imaginary (c'') part of the complex specific heat capacity and the tan δ were determined as a function of temperature, as shown in Fig. 3.

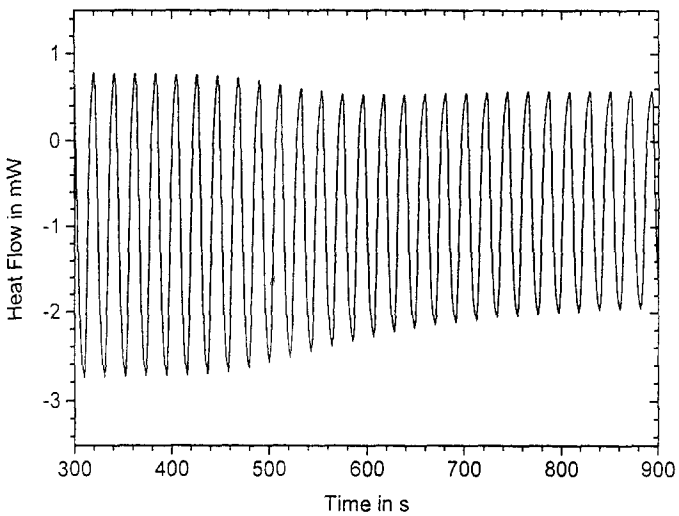

Fig. 2 Modulated heat flow according to the temperature program in Fig. 1 in the glass transition region of PVAc. Sample mass 11.1 mg

During every period of the chosen temperature program the underlying temperature increases by a small step. Most measurements in this paper were carried out with a basic step of the temperature program as follows:

heating from T_o to T_o+2 K (rate β);
immediate cooling for 1.5 K from T_o+2 K to T_o+0.5 K (rate β′).

The heating rate β varied in the range 20 K min^{-1} to 0.08 K min^{-1}, the cooling rate β′ was calculated under the restriction that the time for cooling equals that for heating, which resulted in cooling rates of –15 K min^{-1} to –0.06 K min^{-1}. The temperature amplitude T_a equals 0.6 K for this temperature–time-program.

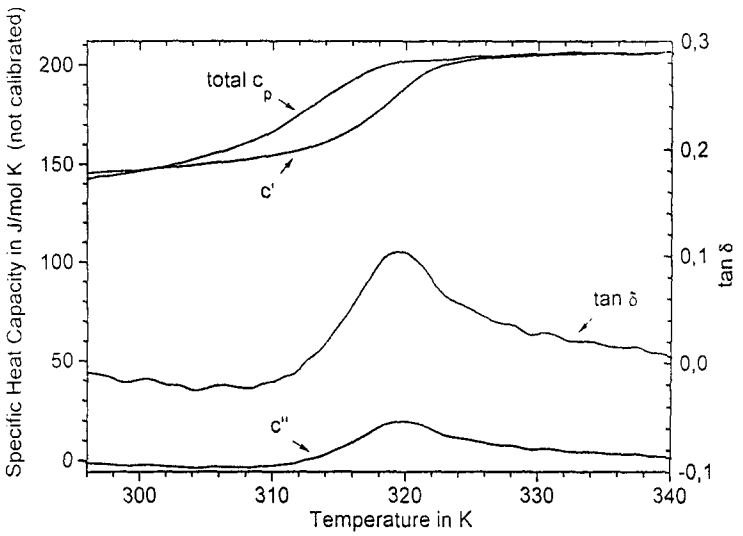

Fig. 3 Specific heat capacities in the glass transition region of PVAc determined from the heat flow from Fig. 2 and the temperature program in Fig. 1 according to equations (1–3) and the loss tangent according to Eq. (4). $\nu = 0.04$ Hz; $T_a = 0.6$ K; $< \beta > = -1.2$ K min^{-1}; $m_p = 11.1$ mg

This basic step results in an increase of the underlying temperature of $\Delta T_p = 0.5$ K during the time of one modulation period. An underlying heating rate $< \beta >$ can be introduced with

$$< \beta > = \frac{\Delta T_p}{t_p} \tag{7}$$

Due to the temperature increase of 0.5 K during one modulation period there is a strong relation between modulation frequency and underlying heating rate $< \beta >$. From the range of the heating rate β and the first ramp of 2 K (half of the modulation period) a frequency range from 0.08 Hz to 0.0003 Hz and an underlying heating rate $< \beta >$ from 2.5 K min^{-1} to 0.01 K min^{-1} can be obtained. Other temperature–time programs results in different values. For cooling experiments the sign of the temperature increments can be inverted (–2 K; +1.5 K).

Because of the temperature step of 0.5 K per period, a total c_p (like in normal DSC experiments) can be determined by averaging the measured modulated heat flow. For the total c_p the corresponding time scale depends on the underlying cooling or heating rate $< \beta >$ associated with the underlying temperature. In Fig. 3 the different specific heat capacities are shown for PVAc in the glass transition region. The shift along the temperature axis between total c_p and c' results from the different time scales of both experiments. This is in agreement with the cooling rate dependence of the glass transition temperature. We have to

recognize that we get information from two independent experiments during one Temperature Modulated DSC experiment. At first, we observe the entropy retardation [21] in the supercooled liquid using the deconvolution of the complex heat capacity from the modulated heat flow. One gets the typical picture for the temperature dependence of a complex compliance in the glass relaxation region. In Fig. 4, the same is shown for the complex dielectric function. A step in the real component and a broad peak in the imaginary component is observed. The corresponding time scale is that of the perturbation (modulation period; frequency) [6, 7]. In addition we observe the freezing of molecular motion during the thermal glass transition (vitrification) due to the underlying cooling process (total c_p). The corresponding time scale depends, as in standard DSC scans, on the underlying cooling rate $< \beta >$. The reason for both processes is the glass relaxation process and, therefore, both are strongly associated [21]. Because the retardation process in the complex heat capacity is observed in a quasi equilibrium state (supercooled liquid at temperature $> T_g$), it is for an amorphous sample largely independent of the cooling or heating conditions, as well as on the thermal history [6, 7]. The normal glass transition (vitrification), in contrast, is strong dependent on the thermal history and there are differences between cooling and heating scans. This is mainly due to the fact that vitrification is the change from a quasi equilibrium (supercooled liquid) to a non equilibrium (glassy) state. Measurements of the glass relaxation not influenced by vitrification require a sufficiently big difference between the time scales of the perturbation and the cooling (or heating) process. This is not only important for temperature modulated differential scanning calorimetric experiments, but

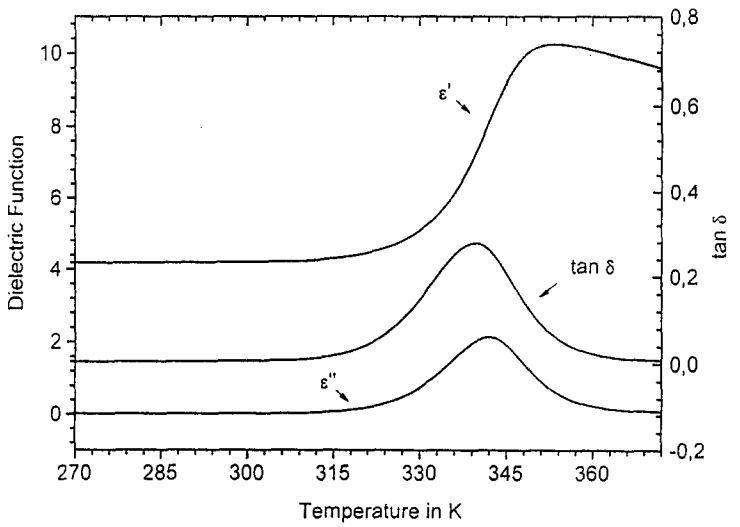

Fig. 4 Complex dielectric function in the glass transition region of PVAc as a function of temperature. $\nu = 1$ kHz; $<\beta> = 0.5$ K min^{-1}

also well known for dielectric [22] and mechanical [23] spectroscopy at low frequencies comparable with the time scale of vitrification. As shown in Fig. 3, there is an overlap in the increase of specific heat at the glass transition obtained from the modulated signal (c') compared with that of vitrification (total c_p) due to the width of the glass transition region, which indicates that although the signals c' and total c_p appear to have different glass transitions, it is still the same effect that is measured. Because of the basic step for the temperature–time-program used for all measurements presented in this paper, there is a constant factor between both time scales. The frequency of the modulation is about 200 times greater than the frequency corresponding to the underlying heating or cooling rate; see below Eqs (9) or (10). Therefore, nearly the same temperature shift between the response of the temperature modulated experiment and vitrification occurs. If there is an influence of the non-equilibrium on the response of the temperature modulated experiment, it is approximately the same for all measurements.

The difference between total c_p and the modulus $|C(\omega)|$ is called nonreversing component [18, 19]. In the case of glass transition it is the difference between two curves related to two different time scales. In this case it is not very useful. For other time dependent processes where the time scale of the elementary process is much faster than the modulation period the nonreversing component include all effects related to excess enthalpies e.g. in the case of cold crystallization or of curing reactions. Then it is a very useful quantity to separate the enthalpies of transition or reaction from changes in the specific heat capacity.

The dielectric measurements were carried out in the frequency range 1 MHz to 0.01 Hz with a BDS 4000 broad band dielectric spectrometer (NOVOCONTROL GmbH). A frequency response analysis is used to extract the complex dielectric function [24]. In the frequency range from 3 Hz to 10^{-5} Hz a step response system was used [25]. The dielectric loss curves in the glass transition region were corrected by the DC-conductivity and by the influence of the local process (secondary process). Details will be published elsewhere [26].

One aim of this work is to compare the dynamic glass transition temperatures obtained by temperature modulated differential scanning calorimetry with that obtained by dielectric spectroscopy. For this reason it is very important to calibrate the temperature read-out of the measuring equipment accurately. That means it is necessary to calibrate the DSC temperature scale for every measuring condition used in this series, as well as to calibrate the dielectric spectrometers. The temperature calibration of the dielectric spectrometers was checked with indium. A sandwich of PTFE – three pieces indium – PTFE was placed between the capacitor plates. The temperature was increased in steps of 0.1 K with a duration of 0.5 h at each temperature, starting 0.5 K below the expected melting point of indium. The melting of indium decreases the distance

between the capacitor plates and the capacity increases. This step in the measured capacity allows us to calibrate the dielectric spectrometers similar to the DSC. The observed difference between the temperature scales of the DSC and the dielectric spectrometers is less than 0.5 K for the heating rates used.

The DSC was calibrated in the standard mode with indium and lead and in the scan-scan mode with the smectic A to nematic transition [27] of 4-cyano-4'-octyloxy-biphenyl [28]. The rate dependence of the temperature calibration, including cooling mode, was independently estimated for both modes with the liquid crystal transition. The heat flow was not calibrated. A calibration procedure will be described elsewhere [29]. The temperature of the heat sink was well stabilized to perform measurements (empty pan and sample run) over times up to 5 days for each run.

The samples under investigation were:
poly(vinyl acetate) (PVAc); M_w =407.000; dried at 450 K for 2 h
crystallizable poly(ether ether ketone) VICTREX® 381 G
poly(ethylene terephthalate) (PET); M_w =23.000.

The materials were melt pressed. The sample thickness was 0.15 mm the diameter of the rods 30 mm. These samples were used for the dielectric experiments and for the calorimetric ones, rods of 5 mm were cut. The sample weight was about 10 mg.

Results

First we want to compare the calorimetric measured dynamic glass transition with that of dielectric experiments. For both experiments we have to find corresponding measured quantities. In correspondence with the linear response theory we select the temperature of the maximum of the imaginary part of the compliance ($c''(T)$; $\varepsilon''(T)$) at a given frequency (temperature dispersion) as the characteristic temperature for the relaxation process. An analogous property is the frequency of the maximum of the imaginary part of the compliance ($c''(\omega)$; $\varepsilon''(\omega)$) at a given temperature (frequency dispersion). Neglecting problems with the influence of the non-equilibrium during the measurements, the pairs (frequency and temperature of the maximum) are the same for both dispersion measurements (temperature–time equivalence). The same result can be observed in the case of symmetric loss peaks from the half-step of the real part of the compliance ($c'(T)$; $\varepsilon'(T)$ or $c'(\omega)$; $\varepsilon'(\omega)$). In the following we discuss the temperature of the maximum of $c''(T)$ at different modulation frequencies ($T_g(\nu)$) and the frequency of the maximum of $\varepsilon''(\nu)$ at different measuring temperatures ($\nu_m(T)$).

With the help of the modified Perkin Elmer DSC-7 we were able to measure the complex heat capacity of PVAc in the frequency range 0.08 Hz to

0.0003 Hz. The reciprocal of the frequency dependent dynamic glass transition temperature $1/T_g(\nu)$ was plotted against the logarithm of the modulation frequency lg(ν) in an activation-plot; Fig. 5. The temperature dependent maximum frequencies $\nu_m(T)$ from dielectric spectroscopy in the frequency range 10^6 Hz to 10^{-5} Hz for the same sample are also shown.There is a significant difference between the results from TMDSC and dielectric spectroscopy. The points from TMDSC are located about one half order of magnitude lower than that from dielectric spectroscopy. The shift along the reciprocal temperature axis corresponds to about 2 K. This is significant greater than the observed differences between the temperature scales of the DSC and the dielectric spectrometers.

The points are fitted with a Vogel-Fulcher-Tamann equation (VFT) [30].

$$\lg\nu = A - \frac{B}{T - T_0} \tag{8}$$

where A and B are constants and T_0 is the Vogel temperature.

The insertion in Fig. 5 shows the entire frequency range used for the calculation of the fit parameters. The parameters from the dielectric points are: A = 11.7; B =694 K; T_0 =264 K. A VFT fit to the points from TMDSC results in the parameter set: A =11.7; B =696 K; T_0 =266 K.

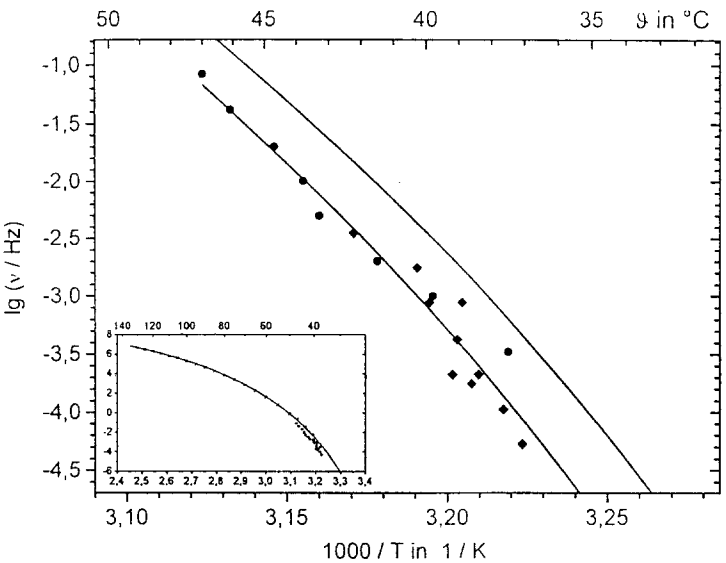

Fig. 5 Activation-plot for PVAc. • - maximum of $c''(T)$; ♦- glass transition temperature from standard DSC, cooling rate transformed into frequency according to Eqs (9) and (10); × - maximum of $\varepsilon''(\nu)$. The insertion shows the entire frequency range for the dielectric measurements. The lines represent the VFT-fit curves, fit-parameter see text

For the Temperature Modulated DSC there is an obvious relation between modulation period and modulation frequency and no problems arise constructing the activation-plot. On the other hand, we know that there is also a relationship between cooling rate and observed glass transition temperature [12]. Because both observations result from the same molecular processes, the glass relaxation, there must be a relation between cooling rate and observed relaxation time and therefore also between cooling rate and frequency. From Donth's fluctuation model of glass transition a rule to transform cooling rates into frequencies was derived [13, 31]:

$$\nu = \frac{\beta}{2\pi a \delta T} \tag{9}$$

where β is the cooling rate, δT is the mean temperature fluctuation (in the order of 2 K [13, 32]) and a is a constant in the order of 1 [13, 33].

From the dislocation concept of glass transition [14] another formula for the transformation results:

$$\nu = \frac{\beta}{2\pi 15\ \mathrm{K}} \tag{10}$$

With the help of temperature modulated calorimetry we are able to test these formulas directly. To compare the glass transition temperature T_g from cooling experiments with that from TMDSC we measured the dried PVAc sample in the standard DSC mode as well. The measurements were performed as following: Annealing the sample at T_g+30 K; cooling with the rate under investigation; immediately heating with the same rate. From the cooling scan as well as from the heating scan the fictive temperature T_f was determined. The fictive temperature from the heating scan equals the glass transition temperature on cooling the sample without annealing periods between cooling and heating [34].

The temperature scale of the DSC was calibrated for every heating and cooling rate under investigation with the help of the liquid crystal transition, see above. Because of the thermal lag there is a rate dependent difference between the glass transition temperature obtained from cooling scans and that obtained from heating scans [35]. It is less than 3 K at 20 K min^{-1}, and negligible for rates lower than 2.5 K min^{-1}. To reduce the influence of the thermal lag on the determined glass transition temperatures and the number of points in Fig. 5, the average value of the glass transition temperatures from cooling and heating is plotted for every rate.

The transformation of cooling rate to frequency were performed according to Eq. (10). The same transformation results from Eq. (9). The mean temperature fluctuation $\delta T = 2.5$ K of PVAc was determined as half of the width of the

glass transition interval of the real part of the complex heat capacity $c'(T)$ according to [13, 32]. The constant was determined as $a = 6$. The identical value was obtained from amorphous PEEK. The VFT-fit from the TMDSC points is extrapolated to the frequency of the standard DSC measurements. Which gives an equally good fit.

To get information, if there is really an influence of the mean temperature fluctuation δT on the transformation of cooling rates to frequency (Eq. (9)), or not (Eq. (10)) it is useful to investigate samples with expected differences in the mean temperature fluctuation δT. As shown in [36] the geometrical restriction of the glass forming regions in semicrystalline polymers results in a significant increase of the mean temperature fluctuation δT with decreasing width of the amorphous regions. We used semicrystalline PEEK, annealed for 2 h at 483 K, to investigate the influence of the mean temperature fluctuation on the transformation from cooling rate to frequency (Fig. 6).

In Fig. 7 the activation-plot for a semicrystalline sample is shown. The fit through the experimental points is less accurate than in PVAc due to the smaller frequency range and fewer experimental data points. A difference between TMDSC and dielectric spectroscopy of about one order of magnitude is observed. To bring the points from standard cooling experiments in coincidence with that of TMDSC is only possible with the help of Donth's formula (Eq. (9)). The mean temperature fluctuation $\delta T = 8$ K was again determined as half of the width of the glass transition interval (Fig. 6) of the real part of the complex heat capacity $c'(T)$ according to [32]. The constant was again determined as $a = 6$. The product $a^*\delta T = 48$ K is significantly greater than the 15 K

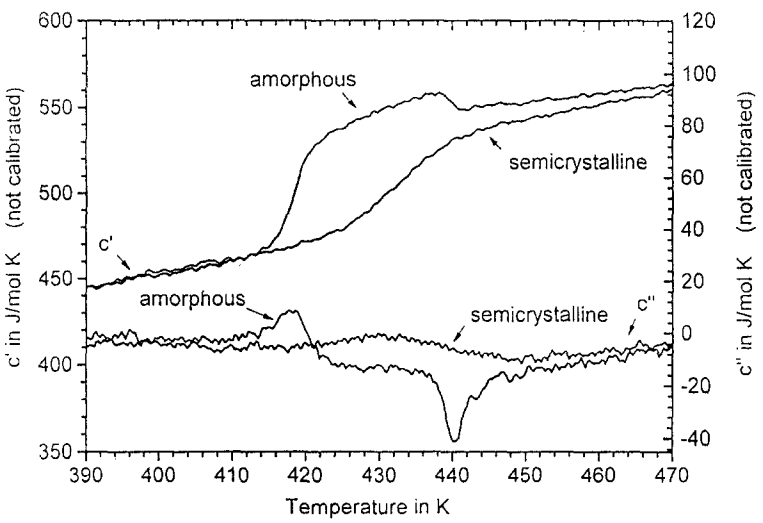

Fig. 6 Complex specific heat capacity of amorphous and semicrystalline (see text) PEEK. $\nu = 0.02$ Hz; $T_a = 0.6$ K; $< \beta > = 0.6$ K min^{-1}; $m_p \approx 3$ mg

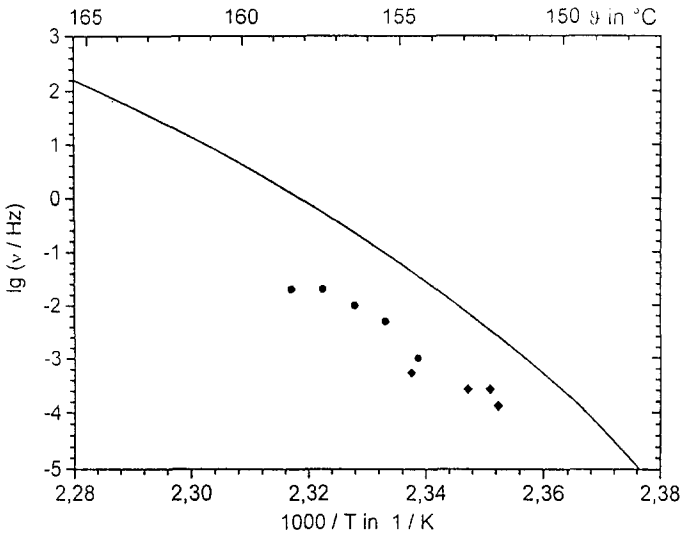

Fig. 7 Activation-plot for semicrystalline PEEK. •-maximum of $c''(T)$; ♦-glass transition temperature from standard DSC, cooling rate transformed into frequency according to Eqs (9); the line represent the VFT-fit curve to the results from dielectric measurements (maximum of $\varepsilon''(\nu)$) [26]

proposed by Stoll exclusively for PVAc [14]. A VFT-fit to the points from calorimetry was not performed because of the scatter and the small number of points.

Comparing the glass transition of semicrystalline polymers with that of amorphous samples, the problem of curve shape arises. From standard DSC investigations, as well as from dielectric spectroscopy, it is well known that the glass transition in semicrystalline polymers is much broader than in amorphous polymers. As shown in [36, 37] there is a relation between the thickness of the mobile amorphous regions and the width of the glass transition interval. Especially the high temperature side of the glass transition is broadened if the geometrical restriction increases as the thickness of the amorphous regions decreases. On the other hand, the low temperature region of the glass transition was only little affected by the restrictions. The same was observed from dielectric experiments.

In Fig. 8 the normalized imaginary part of the dielectric function $\varepsilon''(\nu)$ for amorphous and for semicrystalline PET is shown. The PET was annealed for 3 h at 433 K. For details of the crystalline structure see [38]. To compare the response from an amorphous sample in the glass transition region with that of a semicrystalline one, it is necessary to normalize the response according to the mobile amorphous fraction [3]:

$$\varepsilon''(\nu)_{\text{norm}} = \frac{\varepsilon''(\nu)}{\Delta\varepsilon'/\Delta\varepsilon'_{\text{am}}} \tag{11}$$

where $\Delta\varepsilon'$ is the observed step in the real part of the dielectric function and $\Delta\varepsilon'_{\text{am}}$ is the step in the real part of the dielectric function of a totally amorphous sample. For the semicrystalline sample under investigation $\Delta\varepsilon'=0.8$ and $\Delta\varepsilon'_{\text{am}}=1.65$.

The temperature modulated calorimetry allows us to investigate the curve shape of the heat capacity in an equilibrium state as in the case of dielectric spectroscopy. Therefore, we can prove if there really is a broadening of the relaxation process or if the broadening of the c_p curves results from differences in vitrification of different parts of the sample due to different coupling to the crystalline regions.

To compare frequency dispersion with temperature dispersion measurements we have to remember that high frequency correspond to low temperature and vice versa [21]. In Fig. 9 the normalized imaginary part of the complex heat capacity of the same samples as used for the dielectric spectroscopy is shown. They are also normalized with respect to the mobile amorphous fraction [3]:

$$c''(T)_{\text{norm}} = \frac{c''(T)}{\Delta c'/\Delta c'_{\text{am}}} \tag{12}$$

where $\Delta c'$ is the step in the real part of the specific heat capacity of the semicrystalline sample with a value of $\Delta c'=23$ J mol^{-1} K^{-1}; and $\Delta c'_{\text{am}}$ is the step in

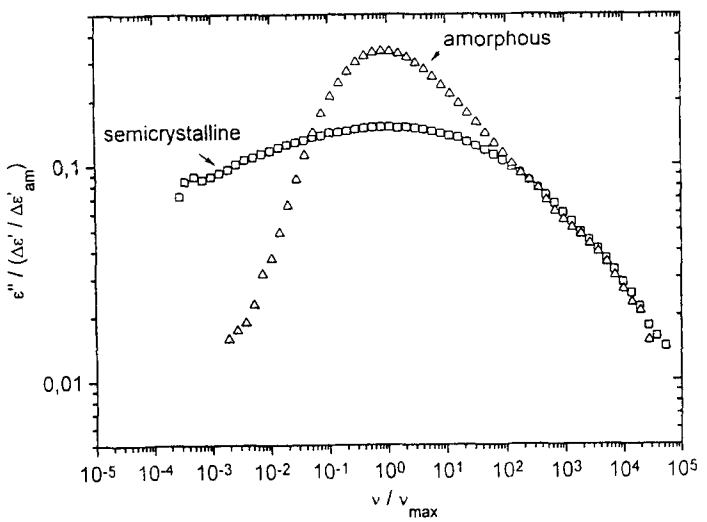

Fig. 8 Normalized imaginary part of the dielectric function (Eq. (11)) in the glass transition region of amorphous and semicrystalline (see text) PET. The frequency axis is normalized to the peak position

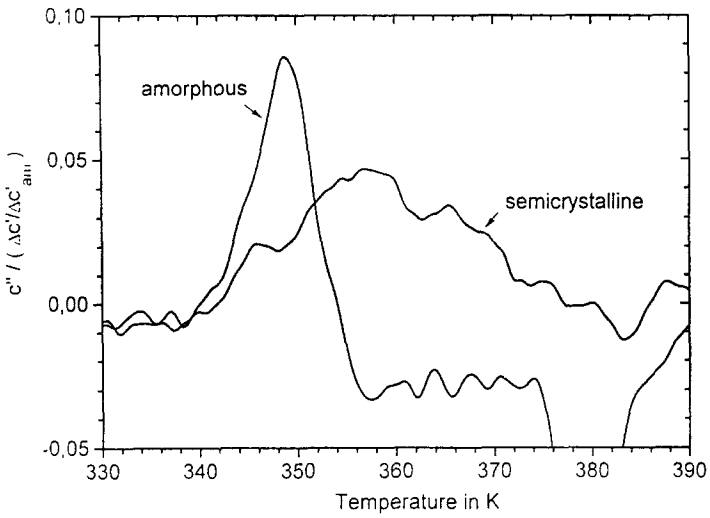

Fig. 9 Normalized imaginary part of the specific heat capacity (Eq. (12)) in the glass transition region of amorphous and semicrystalline (see text) PET. $\nu = 0.02$ Hz; $T_a = 0.6$ K; $<\beta> = 0.6$ K min^{-1}; $m_p \approx 3$ mg

the real part of the specific heat capacity of the totally amorphous sample, $\Delta c'_{am} = 65$ J mol^{-1} K^{-1}.

Because of the very low magnitude of c'', there are some irregularities. The negative c'' in the region of cold crystallization is an interesting observation, but not subject of this paper. Why the c'' is negative between glass transition and cold crystallization is not understood and may only be the result of experimental error [39].

Due to the very small steps in the real parts of the compliance, the normalized curves for the semicrystalline sample are magnified and therefore appear to be noisy. But in both figures we can observe that the "high frequency/low temperature" side of the glass transition is only slightly affected by the crystalline structure. In contrast the "low frequency/high temperature" side is significantly broader.

Discussion

Temperature modulated calorimetry is an additional possibility to get information on the response of a sample to a small perturbation within the linear response approach. This is of interest in every case where the process under investigation is time dependent. In this paper the focus is on the glass transition as a relaxation phenomenon.

The complex heat capacity obtained from TMDSC within the linear response approach shows the same general behavior as other compliance's. There

is a step in the real part and a broad peak in the imaginary part in the frequency dispersion [16] as well as in the temperature dispersion. In the case of glass transition, the real part of the heat capacity is comparable to the standard heat capacity because of the very small imaginary part. The maximum of $c''(T)$ is in the order of 20 J mol^{-1} K^{-1} for amorphous and 6 J mol^{-1} K^{-1} for semicrystalline PET. The maxima of the loss tangent are of the order of 0.1 and 0.03, respectively. From the dielectric spectroscopy we obtain the same values for the maximum of the loss tangent: 0.1 for the amorphous and 0.03 for the semicrystalline sample.

The different responses (location in the activation plot) to different perturbations including temperature are not quite understand and should be part of future work about the phenomenon of the glass transition. At present the discussion will be from a phenomenological point of view.

First, we compare the results obtained by TMDSC in the frequency range available with dielectric spectroscopy. As shown in Fig. 5 the points from TMDSC result in a trace in the activation-plot comparable with that of dielectric spectroscopy. Both traces show a similar curvature, indicating the cooperative nature of the underlying process. They can be described with the help of a VFT-equation. The significant difference between the two fits is the shift in the VOGEL-temperature T_0. The trace of the TMDSC points is shifted by about one-half order of magnitude to lower frequencies (slower process). The Vogel-temperature T_0 is 2 K higher than for the points from dielectric spectroscopy. As a first result, we can conclude that TMDSC and dielectric spectroscopy detect the same process, the dynamic glass transition. The main sensitivity of the two, however, is different. The response to the temperature disturbance weights slower modes of the molecular movement more than the response to the disturbance of the electrical field. Therefore, the curves are shifted with respect to each other.

Because vitrification is also due to the glass relaxation process, TMDSC gives the opportunity to directly compare the time scale of a vitrification in a linearly cooled sample with that of a cooling experiment in the heat-cool-mode. In Fig. 5 the glass transition temperatures from standard DSC cooling experiments are added to TMDSC data. The cooling rates are transformed according to the formulas given by Stoll [14] and Donth [13]. The trace in the activation-plot is comparable to that from TMDSC. It is curved, and the VFT-fit from the TMDSC experiment also fits these values. The fact that both the DSC and TMDSC values are on one curve indicates that it is really possible to transform cooling rates into frequencies. Vitrification is part of the glass relaxation process and there is no separate description or theory of it necessary.

For amorphous polymers both transformation rules, as shown in Eqs (9) and (10), are equivalent. The remaining question is that of the influence of the mean temperature fluctuation on the transformation proposed by Donth. The evalu-

ation of the Eq. (9) starts from the fluctuation of small cooperatively rearranging regions (CRR). For a given temperature the fluctuation e.g. of the temperature can be described by magnitude (δT) and mean frequency. With decreasing temperature the frequency of the fluctuation decreases. To discuss the relation between mean temperature fluctuation and the step in the heat capacity at glass transition we will use a simple picture. Looking at the temperature range above the glass transition, and cooling the sample with a rate β through the glass transition region, one observes that at high temperatures an averaging over the fluctuation can be performed because the time needed for a small temperature increment, determined by the cooling rate, is longer than the fluctuation period. Then the subsystem contributes to the specific heat capacity.

$$C_p = k\,\overline{\Delta S}^2 \tag{13}$$

With k representing Boltzmann's constant and $\overline{\Delta S}^2$, the mean entropy fluctuation [21].

At low temperatures the time given by the cooling rate is the same, but the fluctuation period is longer and therefore the averaging over the fluctuation is not possible. The subsystem does not contribute to the specific heat capacity. This simple picture permits to describe the behavior change at temperatures close to the glass transition and the step in the specific heat capacity. If the magnitude of the fluctuation is small, this change occurs in a small temperature region (width of the glass transition region) and *vice versa*. For a subsystem with a high magnitude of the temperature fluctuations follows that for a given cooling rate the averaging is possible down to lower temperatures. Because of the temperature–time-equivalence that means the corresponding frequency is lower. As shown by this simple picture, there is a relation between frequency, cooling rate, mean temperature fluctuation, and the width of the glass transition region. Therefore, it is possible to determine the mean temperature fluctuation from the width of the glass transition region, as described in [32].

To support this explanation, a semicrystalline sample (PEEK) was investigated, as shown in Fig. 6. Due to the geometrically restriction of the amorphous regions, the mean temperature fluctuation in this sample should be higher than in an amorphous sample [36]. From the half-width of the glass transition region in the real part of the complex heat capacity, the mean temperature fluctuation $\delta T \approx 8$ K for the semicrystalline sample was determined. This value is about three times greater than that obtained for the amorphous samples. With Eq. 9 and a value of $a = 6$, as determined from amorphous PVAc, the transformation of the cooling rate into frequency is in agreement with the results of TMDSC for the semicrystalline PEEK. In the case of the semicrystalline sample, the product $a^*\delta T = 48$ K. The value is significant higher than the one obtained for the amorphous samples which is of the order of 15 K. This shows

that the simple picture for the fluctuation model of the glass transition [13] is valid.

Because of the complex morphology of semicrystalline polymers the question arises whether the observed glass transition results from one relaxation process broadened due to geometrical restriction, or from the superposition of different glass transitions with different glass transition temperatures. If the second argument is valid, then there is no opportunity to determine mean temperature fluctuations from the width of the glass transition region in semicrystalline polymers. Therefore, we investigated the shapes of the peaks in both the imaginary part of the dielectric and the heat capacity functions. As shown in Fig. 8, the peak of the imaginary part of the dielectric function is significantly broader when compared to the one of amorphous PET. But this broadening can be observed only for the low frequency side of the peak. The high frequency side is not influenced by the crystalline structure. According to Schönhals [40] the high frequency side is related to short-mode length molecular motions (short distance fluctuations). These are the local motions which are not influenced by the geometrical restrictions of the crystals because of their short mode length. The mode length is much shorter than the dimension of the remaining mobile amorphous regions in the semicrystalline sample. For these molecular motions it is unimportant if there are crystals located at a relatively long distance, compared with the mode length or not. Therefore, there is no difference between semicrystalline and amorphous PET on the high frequency side of the peak. The molecular motions related to the low frequency side of the peak are influenced by the crystalline structure. The motions detected at low frequencies are associated with long mode length (long distance fluctuations) comparable with the dimension of the mobile amorphous regions in the semicrystalline sample. Because of the geometrical restrictions by the crystals, the mode length is confined to the geometrical length. To realize all the molecular movements which are necessary to result in the contribution of the 11 J mol^{-1} K^{-1} per mobile bead [2] to Δc_p, the molecules have to find other ways than that with the long mode length. That means, the conformational changes will be performed in a way that needs more time. In Fig. 8 we observe a drastic broadening of the side related to these modes for the semicrystalline sample. For this discussion we have to recognize that at the measuring temperature the mobile amorphous part of the sample is in the liquid state. Therefore, the Δc_p reaches the value of 11 J mol^{-1} K^{-1} per mobile bead.

If the observed glass relaxation results from the superposition of different relaxation processes with different frequencies of the maximum of the complex part of the dielectric function, there is no possibility to construct a peak with constant high frequency flank and significantly broader low frequency flank.

Because of the temperature–time-equivalence we can discuss the same for a temperature scan. In Fig. 9 the complex heat capacity for the amorphous as

well as for the semicrystalline PET sample is shown. It can be seen that the low temperature flank for both samples is only little influenced by the crystalline structure. In contrast, the high temperature flank is much broader for the semicrystalline sample. This is in agreement with the discussion for the dielectric measurement because low temperature corresponds to high frequency and *vice versa*.

As shown, there are good arguments that the width of the glass transition region is related to the mean temperature fluctuation and does not result from the superposition of different glass transitions in semicrystalline samples.

Conclusion

Temperature modulated calorimetry is an interesting new method which allows us to compare calorimetric results from the glass transition with that of typical dynamic measurements like dielectric or mechanic spectroscopy. It should be possible to solve some of the basic questions concerning the glass transition. Our very first results are in good agreement with the suggestions of the fluctuation model proposed by Donth [13, 31] and with the general rules given by Wunderlich [2]. In the future, we will further investigate the glass transition in semicrystalline systems (polymers and low molecular weight materials) to study the influence of the geometrical restriction on the glass relaxation especially on the complex heat capacity.

In the case of glass transitions we can discuss the complex heat capacity within the linear response approach. For other time dependent events like chemical reactions, phase transitions and others, the picture is not as simple and further work is necessary.

References

1 B. Wunderlich and J. Grebowicz, Adv. Polymer Sci., 60/61 (1984) 1.
2 B. Wunderlich, J. Phys. Chem., 64 (1960) 1052.
3 H. Suzuki, J. Grebowicz and B. Wunderlich, Brit. Polym. J., 17 (1986) 1.
4 B. Wunderlich, Assignment of the Glass Transition, ASTM STP 1249. Ed. R.J. Seyler (American Society for Testing and Materials, Philadelphia 1994 pp. 17.
5 B. Wunderlich, Progr. Colloid Polym. Sci., 96 (1994) 22.
6 A. Boller, C. Schick and B. Wunderlich, Proc. 23rd NATAS Conference, Toronto 1994 p. 1.
7 A. Boller, C. Schick and B. Wunderlich, Thermochim. Acta, (1996) (in press).
8 R. Kubo, Rep. Prog. Phys., 29 (1966) 255.
9 L. D. Landau and E. M. Lifshitz, Statistical Physics, Vol. 12 Pergamon Press, Oxford 1980.
10 D. H. Jung, T. W. Kwon, D. J. Bae, I. K. Moon and Y. H. Jeong, Meas. Sci. Technol., 3 (1992) 475.
11 J. E. K. Schawe, Thermochim. Acta, 183 (1995) 183.
12 B. Wunderlich, D. M. Bodily and M. H. Kaplan, J. Appl. Phys., 35 (1964) 95.
13 E. Donth, Glasübergang, Akademieverlag, Berlin 1981.
14 W. Heinrich and B. Stoll, Progr. Colloid Polym. Sci., 78 (1988) 37.
15 P. F. Sullivan and G. Seidel, Phys. Rev., 173 (1968) 679.

16 N. O. Birge and S. R. Nagel, Rev. Sci. Instrum., 58 (1987) 1464.
17 M. Reading, D. Elliot and V. L. Hill, J. Thermal Anal., 40 (1993) 949.
18 M. Reading, Trends Polym. Sci., 8 (1993) 248.
19 B. Wunderlich, Y. M. Jin and A. Boller, Thermochim. Acta, 238 (1994) 277.
20 A. Boller, Y. Jin and B. Wunderlich, J. Thermal Anal., 42 (1994) 307.
21 E. Donth, Relaxation and Thermodynamics in Polymers: Glass Transition, Akademie Verlag, Berlin 1992.
22 A. Schönhals and E. Donth, Acta Polymerica, 37 (1986) 475.
23 G. Vigier and J. Tatibouet, Polymer, 34 (1993) 4257.
24 F. Kremer, D. Boese, G. Meier and E. W. Fischer, Progr. Colloid Polym. Sci., 80 (1989) 129.
25 A. Schönhals, Acta Polymerica, 42 (1991) 149.
26 J. Dobbertin, Thesis, University of Rostock 1995.
27 G. W. H. Höhne, J. Schawe and C. Schick, Thermochim. Acta, 221 (1993) 129.
28 A. Hensel and C. Schick, (1996) in preparation.
29 J. Schawe and M. Margulies, in preparation.
30 H. Vogel, Phys. Z., 22 (1921) 645.
31 E. Donth, J. Non. Cryst. Solids, 53 (1982) 325.
32 K. Schneider, A. Schönhals and E. Donth, Acta Polymerica, 32 (1981) 471.
33 C. Meischner, B. Greiner, P. Hauptmann and E. Donth, Acta Polymerica, 37 (1986) 453.
34 M. Richardson, Comprehensive Polymer Sience, Vol. 1. Ed. G. Allen, Pergamon Press, Oxford 1989, p. 867.
35 J. Schawe and C. Schick, Thermochim. Acta, 187 (1991) 335.
36 C. Schick and E. Donth, Physica Scripta, 43 (1991) 423.
37 C. Schick, J. Wigger and W. Mischok, Acta Polymerica, 41 (1990) 137.
38 C. Schick, F. Fabry, U. Schnell, G. Stoll, L. Deutschbein and W. Mischok, Acta Polymerica, 39 (1988) 705.
39 J. E. K. Schawe and G. W. H. Höhne, J. Thermal Anal., (this issue).
40 A. Schönhals and E. Schlosser, Coll. Polym. Sci., 267 (1989) 125.